European Journal of Medicinal Chemistry 94 (2015) 386–396

Contents lists available at ScienceDirect

European Journal of Medicinal Chemistry

journal homepage: http://www.elsevier.com/locate/ejmech

Original article

Design of a serotonin 4 receptor radiotracer with decreased lipophilicity for single photon emission computed tomography

Nathalie Fresneau [a], Noé Dumas [b], Benjamin B. Tournier [b], Christine Fossey [c], Céline Ballandonne [c], Aurélien Lesnard [c], Philippe Millet [b], Yves Charnay [b], Thomas Cailly [c], Jean-Philippe Bouillon [a, *], Frédéric Fabis [c, *]

[a] Normandie Univ., COBRA, UMR 6014 et FR 3038, Univ. Rouen, INSA Rouen, CNRS, 1 Rue Tesnière, F-76821 Mont-Saint-Aignan Cedex, France
[b] Hôpitaux Universitaires de Genève, Département de Santé Mentale et de Psychiatrie, Service de Psychiatrie Générale, Unité des Biomarqueurs de Vulnérabilité, Chemin du Petit-Bel-Air, 2, CH-1225 Genève, Switzerland
[c] Normandie Univ., Université de Caen Basse-Normandie, CERMN (EA 4258, FR CNRS 3038 INC3M, SF 4206 ICORE), UFR des Sciences Pharmaceutiques, Bd Becquerel, F-14032 Caen, France

ARTICLE INFO

Article history:
Received 3 June 2014
Received in revised form
5 March 2015
Accepted 6 March 2015
Available online 9 March 2015

Keywords:
Molecular imaging
SPECT
Radiolabeling
Iodine
5-HT
Serotonin

ABSTRACT

With the aim to develop a suitable radiotracer for the brain imaging of the serotonin 4 receptor subtype (5-HT$_4$R) using single photon emission computed tomography (SPECT), we synthesized and evaluated a library of di- and triazaphenanthridines with lipophilicity values which were in the range expected to favour brain penetration, and which demonstrated specific binding to the target of interest. Adding additional nitrogen atoms to previously described phenanthridine ligands exhibiting a high unspecific binding, we were able to design a radioiodinated compound [^{125}I]**14**. This compound exhibited a binding affinity value of 0.094 nM toward human 5-HT$_4$R and a high selectivity over other serotonin receptor subtypes (5-HTR). *In vivo* SPECT imaging studies and competition experiments demonstrated that the decreased lipophilicity (in comparison with our previously reported compounds **4** and **5**) allowed a more specific labelling of the 5-HT$_4$R brain-containing regions.

© 2015 Elsevier Masson SAS. All rights reserved.

1. Introduction

Serotonin (5-hydroxytryptamine, 5-HT) is a neurotransmitter interacting with at least 15 receptor subtypes (5-HTR) all being GPCRs (G-protein coupled receptors) except the serotonin 3 receptor (5-HT$_3$R) [1]. Among these receptors, the serotonin 4 receptor (5-HT$_4$R) was first identified in 1988 [2] and found to be expressed in both peripheral and central nervous system (CNS) where its activation *in vivo* causes the production of cyclic adenosine mono phosphate (cAMP) [3], activation of Ca^{2+} channels [4], inhibition of K^+ channels [5] and activation of the rap1-rac pathway [6]. Discovery and pharmacological evaluation of potent and selective ligands for 5-HT$_4$Rs [7], have led to a better knowledge of their role in physiological and pathological conditions. Therefore, peripheral 5-HT$_4$Rs have been shown to play important role in gastrointestinal disorders [8,9] and heart failures [10–12] while brain 5-HT$_4$Rs have been shown to play a role in cognition [13], learning and memory processes [14], and more recently in neuropsychiatric disorders such as Alzheimer's disease [15,16], feeding disorders [17], and depression [18].

Besides pharmacological studies with specific ligands, imaging studies using positron emission tomography (PET) and single photon emission computed tomography (SPECT) have now emerged as valuable tools for *in vivo* study of biological systems and especially for neurotransmission systems. Despite these imaging techniques being used in both clinical studies and drug discovery programs [19,20], research in this field remains strongly hampered by the low availability of suitable radioligands. To date, in the case of 5-HT$_4$R radiotracers, the ideal candidate has not been found yet and even if [^{123}I]**1** ([^{123}I]SB-207710) [21], [^{11}C]**2** ([^{11}C]SB-207145) [22,23] and [^{18}F]**3** ([^{18}F]MNI-698) [24,25] (Chart 1) have been described, their use remains restricted due to their fast metabolism and/or short half-life of the chosen isotope. Nevertheless, these structurally similar radiotracers have been successfully used in minipig for the determination of radioligand metabolism and binding kinetics [26], and in the human brain for quantitative measurements of 5-HT$_4$R [27–32].

* Corresponding authors.
E-mail addresses: jean-philippe.bouillon@univ-rouen.fr (J.-P. Bouillon), frederic.fabis@unicaen.fr (F. Fabis).

http://dx.doi.org/10.1016/j.ejmech.2015.03.017
0223-5234/© 2015 Elsevier Masson SAS. All rights reserved.

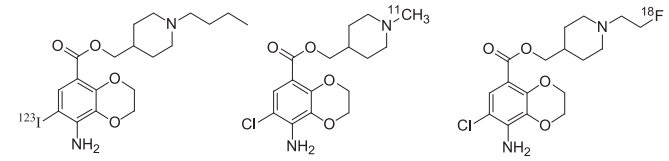

Chart 1. Literature 5-HT$_4$R PET and SPECT radiotracers.

Recently, our group has reported the synthesis and structure–affinity relationships (SAR) of several high affinity 5-HT$_4$R receptor antagonists based on the azaphenanthridine scaffold from which three iodinated potential SPECT tracers have been designed [33]. Among these antagonists, **4**–**6** were successfully radiolabeled with ^{125}I (Chart 2). Their evaluation as SPECT imaging agents showed non-specific binding to brain sections in *ex vivo* experiments (unpublished results), making them unsuitable for further development as potential SPECT radiotracers. In the CNS, the development of suitable radiotracers is constrained by the specific pharmacokinetic properties an ideal candidate should possess [34]. Of these, passage through the blood brain barrier (BBB) is a prerequisite, and low levels of non-specific binding are also highly desirable to achieve good signal to noise ratios. Lipohilicity plays an important role in both of these: ideally the ligand should possess a logP value between 2.0 and 3.5 to pass through the BBB [35–37] and lower non-specific binding is also associated with lower lipophilicity [35,38]. Assuming that the unspecific labelling observed with [^{125}I]**4**–**6** should be the consequence of their high lipophilicity (logD = 4.2–4.3 for compounds **5** and **6**), we designed a set of analogues with decreased lipophilicities by adding nitrogen atoms within the tricyclic framework. The introduction of nitrogen atom in aromatic structures has often been used as a successful strategy to decrease lipophilicity [39,40]. We report here the results of this study, which has led to the discovery of an iodinated ligand [^{125}I]**14**, exhibiting a higher 5-HT$_4$R binding affinity (compared to our previously reported compounds **4**–**6**), a good selectivity and a reduced lipophilicity.

2. Results

2.1. Chemistry

The azaphenanthridinones **9a**–**g,j-o** were prepared as previously described [42,43]. Azaphenanthridinones **9h,i** were obtained from 3-chloropyrazine-2-carbonitrile in a two-step sequence involving a Suzuki cross-coupling followed by a KOH mediated anionic ring closure (Scheme 1).

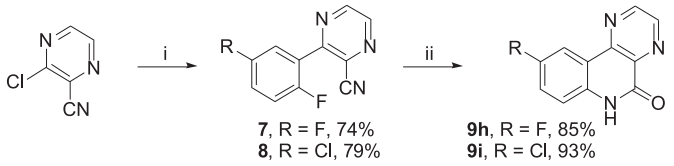

Scheme 1. Synthesis of **9h,i**. Isolated yields, reagents and conditions: (i) 2,5-difluorophenylboronic acid [42] or 5-chloro-2-fluorophenylboronic acid [42], Na_2CO_3, $Pd(OAc)_2$, *S*-Phos, DME/H_2O, heating overnight or 25 min, reflux; (ii) KOH, *t*-BuOH, sealed tube, 1.5 h, 150 °C.

In order to prepare the final 5-HT$_4$R ligands, azaphenanthridinones **9a**–**o** were first reacted with the Vilsmeier–Haack reagent affording the chlorimine derivatives, which were then substituted with (1-propylpiperidin-4-yl)methanol to give compounds **10a**–**o** (Table 1).

The iodine atom was introduced on the tricyclic framework using a silicon/iodine exchange (Scheme 2) [33]. Thus, by reacting 3-chloropyrazine-2-carbonitrile and 2-fluoro-3-trimethylsilylphenylboronic acid in a Suzuki cross-coupling reaction trimethylsilylbiaryl derivative **11** was obtained in 90% yield. The TMS group was then replaced by iodine using ICl and the resulting iodobiaryl derivative **12** was then cyclized using KOH anionic ring closure to afford 7-iodopyrazino[2,3-*c*]quinolin-5(6*H*)-one **13** in 73% yield. The corresponding iodo-pyrazino[2,3-*c*]quinoline **14** was then obtained using the chlorination/S$_N$Ar sequence described above.

2.2. Synthesis of radioligand

Prior to radioiodination, a stannylated precursor was directly prepared from **14** using tin–iodine exchange mediated by Pd(0) (Scheme 3). Thus, by reacting **14** with hexa-*n*-butylditin, $Pd(OAc)_2$, PPh_3 in PhMe/H_2O at 90 °C for 16 h, stannylated precursor **15** was obtained in 45% yield. Radioiodination of **15** was then performed under acidic conditions using Na^{125}I as the radioactive iodine source and H_2O_2 as the oxidant. Therefore, after HPLC purification, [^{125}I]**14** was isolated in a 88.7 ± 2.4% radiochemical yield and a specific radioactivity of 61050 ± 7844 GBq mmol^{-1} (mean ± SD of 3 runs).

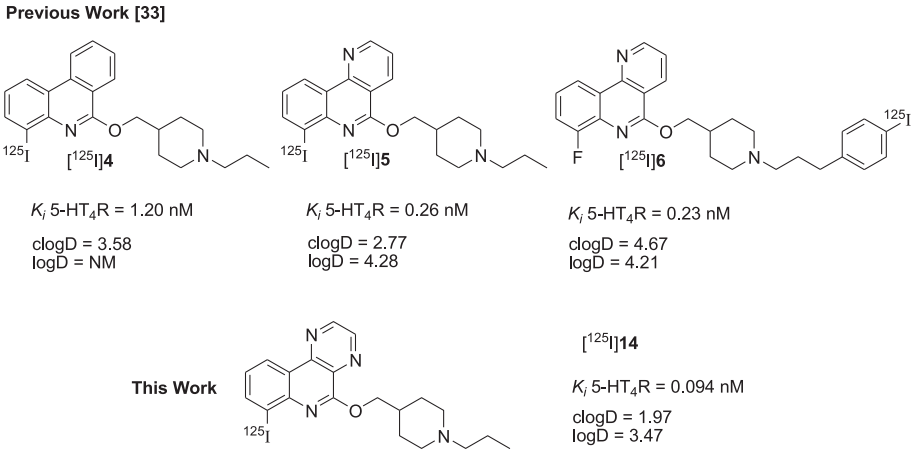

Chart 2. Radioiodinated phenanthridine-based 5-HT$_4$R ligands. clogD = calculated logD (pH = 7.4) using MarvinSketch 5.2.6. LogD = measured logD (pH = 7.4) using chromatographic hydrophobicity index [41]. NM = not measured. K_i measured on human 5-HT$_4$R [33].

Table 1
Synthesis of (polyaza)phenanthridines **10a**–**o**.[a]

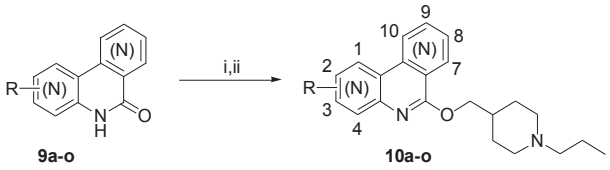

Starting material	N1	N2	N3	R	Product	Yield (%)[b]
9a	1	3	–	–	**10a**	21[c]
9b	1	4	–	–	**10b**	44[c]
9c	1	4	9	–	**10c**	10
9d	2	4	–	–	**10d**	32
9e	3	4	–	–	**10e**	42[c]
9f	4	7	10	–	**10f**	50
9g	7	10	–	–	**10g**	61
9h	7	10	–	2-F	**10h**	67
9i	7	10	–	2-Cl	**10i**	57
9j	7	10	–	3-F	**10j**	67
9k	7	10	–	3-Cl	**10k**	53
9l	7	10	–	4-F	**10l**	80
9m	7	10	–	4-Cl	**10m**	77
9n	7	10	–	4-CF_3	**10n**	71
9o	7	10	–	4-OMe	**10o**	46

[a] Reagents and conditions: (i) $(COCl)_2$, DMF, $CHCl_3$ 2 h, reflux; (ii) (1-propylpiperidin-4-yl)methanol, LHMDS, DMF, overnight, rt.
[b] Isolated yields.
[c] Yields over three steps, see Experimental data for details.

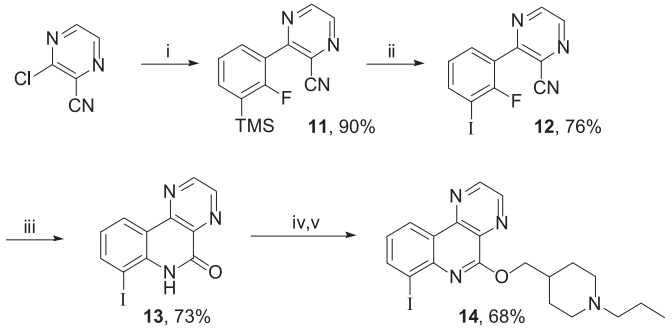

Scheme 2. Synthesis of **14**. Isolated yields, reagents and conditions: (i) 2-fluoro-3-(trimethylsilyl)phenylboronic acid [33], Na_2CO_3, $Pd(OAc)_2$, *S*-Phos, DME/H_2O, 0.25 h, reflux; (ii) ICl, CH_2Cl_2, 4.5 h, rt; (iii) KOH, *t*-BuOH, sealed tube, 1.5 h, 150 °C; (iv) $(COCl)_2$, DMF, $CHCl_3$, 2 h, reflux; (v) (1-propylpiperidin-4-yl)methanol, LHMDS, DMF, overnight, rt.

2.3. 5-HT_4R binding affinity, logD, functional assays and 5-HTRs binding profile

Compounds **10a**–**o** and **14** were screened for their affinity toward 5-HT_4R in guinea pig striatal membranes at 10^{-6} and 10^{-8} M (Table 2). *Ki* values were determined and found to be between 0.04 and 137 nM. Compounds **10g,l,m** and **14** were then chosen for human 5-HT_4R *Ki* determination and were found to exhibit *Ki* values between 0.026 and 0.34 nM. LogD at pH = 7.4 were calculated using MarvinSketch 5.2.6 and measured using chromatographic hydrophobicity index [41]. Compound **14** was evaluated for its functional profile and was found to be an antagonist with a K_B value of 0.18 nM (Table 3). Finally, **14** was screened for its selectivity over a panel of 5-HT receptors, results are depicted in Table 3.

2.4. Imaging experiments

The preclinical evaluation of compound [^{125}I]**14** as a 5-HT_4R SPECT tracer, was performed by injection of 38.9 ± 4.3 MBq of [^{125}I]**14** in rats. Representative SPECT images averaged over 10–60 min post-injection and obtained with [^{125}I]**14** alone or in presence of **16** were shown in Fig. 1. Brain time activity curves of [^{125}I]**14** show higher uptake in limbic regions, enriched in 5-HT_4R, than in cerebellum, a region devoid of 5-HT_4R (Fig. 1D). In the representative SPECT images, the intensity of the [^{125}I]**14** signal in the presence of **16** appeared reduced in the visible limbic regions (striatum, hippocampus and thalamus) as compared to cerebellum (Fig. 1C). *Ex vivo* quantification of [^{125}I]**14** binding alone and in the presence of the 5-HT_4R selective antagonist **16** (RS-39604) [44], to assess the specificity of the 5-HT_4R labelling (Fig. 2), is shown in Table 4. In the presence of **16**, the specific binding of [^{125}I]**14** was reduced in 5-HT_4R containing regions, such as the interpeduncular nucleus (IP, 56.8% binding reduction; $p < 0.01$), brainstem (Bs, 54.7% binding reduction; $p < 0.05$), or striatum (St, 40.7% binding reduction; $p < 0.05$). However, there was less binding inhibition in other regions such as hippocampus (Hip, 26.2% binding reduction; $p < 0.05$).

3. Discussion

In a previous study [33], we have described iodinated phenanthridine-based 5-HT_4R-ligands **4**–**6** to develop 5-HT_4R SPECT radiotracers (Chart 2). Unfortunately, imaging experiments with these compounds revealed high unspecific binding leading to uniform labelling of brain sections. As high lipophilicities are often associated with high non-specific binding, we set out to design less lipophilic compounds by introducing additional nitrogen atoms in the phenanthridine framework. Therefore, a set of di- and triazaphenanthridines derivatives **10a**–**g** with decreased lipophilicities was first synthesized and tested for their affinity in guinea pig 5-HT_4R (Table 2). Among these compounds, diazaphenanthridines **10a,d,e** bearing nitrogen atoms in position 1,3, 2,4 and 3,4 exhibited binding affinities between 12.7 and 137 nM. Interestingly, the 1,4- and 7,10-diazacompounds **10b** and **10g** showed higher binding affinities with the latter exhibiting a subnanomolar K_i value of 0.93 nM on guinea pig and 0.34 nM on human 5-HT_4R. For all these compounds, lipophilicities were first calculated showing clogD values close to 1. Experimental logD were then measured using the chromatographic hydrophobicity index

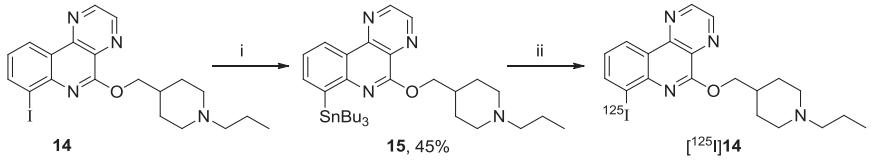

Scheme 3. Synthesis of [^{125}I]**14**. Isolated yields, reagents and conditions: (i) $(Bu_3Sn)_2$, $Pd(OAc)_2$, PPh_3, PhMe/H_2O, 16 h, 90 °C; (ii) Na^{125}I, H_2O_2, EtOH/HCl, 0.33 h, rt.

Table 2
Binding affinities and logD of new 5-HT_4R ligands **10a–o** and **14**.

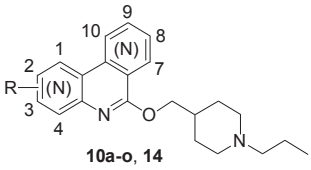

10a-o, **14**

Compd.	N1	N2	N3	R	5-HT_4R % inhbn.[a] (10^{-6} M/10^{-8} M)	5-HT_4R *Ki* ± SD (nM)		clogD[d]	logD[e]
						Guinea pig[b]	Human[c]		
10a	1	3	–	–	100/35	12.7 ± 1.9	NM[f]	1.12	NM
10b	1	4	–	–	104/46	7.87 ± 2.1	NM	0.95	2.22
10c	1	4	9	–	96/16	39.4 ± 4.7	NM	−0.26	1.26
10d	2	4	–	–	94/9	137 ± 35	NM	1.07	1.55
10e	3	4	–	–	100/26	27.8 ± 3.0	NM	0.80	NM
10f	4	7	10	–	100/39	4.84 ± 2.7	NM	0.17	1.27
10g	7	10	–	–	105/86	1.75 ± 0.9	0.34 ± 0.09	1.03	2.38
10h	7	10	–	2-F	100/11	32.3 ± 3.0	NM	1.18	2.78
10i	7	10	–	2-Cl	99/7	52.2 ± 8.0	NM	1.64	3.34
10j	7	10	–	3-F	100/49	4.22 ± 1.1	NM	1.18	2.66
10k	7	10	–	3-Cl	100/2	47.7 ± 9.6	NM	1.64	3.28
10l	7	10	–	4-F	107/100	0.04 ± 0.02	0.029 ± 0.01	1.18	2.51
10m	7	10	–	4-Cl	105/100	0.99 ± 0.1	0.026 ± 0.01	1.64	3.04
10n	7	10	–	4-CF_3	100/49	18.2 ± 8.0	NM	1.92	NM
10o	7	10	–	4-OMe	100/74	2.43 ± 1.0	NM	0.87	2.01
14	7	10	–	4-I	100/87	2.62 ± 1.0	0.094 ± 0.03	1.97	3.47

[a] Inhibition percentages were determined by using guinea pig striatal membrane 5-HT_4R.
[b] Guinea pig striatal membrane 5-HT_4R(Ki ± SD, n = 3).
[c] Human 5-HT_4R (Ki ± SD, n = 2), K_i determinations for *h*5-HT_4R were performed at CEREP. See Experimental section for details.
[d] Calculated logD (pH = 7.4) using MarvinSketch 5.2.6.
[e] LogD (pH = 7.4) measured using chromatographic hydrophobicity index [41].
[f] NM = not measured.

Table 3
Selectivity and functional profile of compound **14**.

Human 5-HTR	% Inhbn. (10^{-6} M)[a]	*Ki* (nM)[b]
5-HT_{1a}	37	NM[d]
5-HT_{1b}	−10	NM
5-HT_{1d}	25	NM
5-HT_{2a}	77	130
5-HT_{2b}	78	100
5-HT_{2c}	88	20
5-HT_3	20	NM
5-HT_{5a}	−6	NM
5-HT_6	28	NM
5-HT_7	23	NM
SERT	48	NM
5-HT_4R functional assay[c]	Antagonist K_B = 0.18 nM	

[a] Inhibition percentages were determined at CEREP. See Experimental section for details.
[b] K_i determinations were performed at CEREP. See Experimental section for details.
[c] Functional assays performed at CEREP. See Experimental section for details.
[d] NM = not measured.

[41]. Although higher logD values between 1.55 and 2.38 were obtained, all these values remained well-correlated to calculated logD. Starting from **10b** and **10g**, we introduced an additional nitrogen atom leading to triazaphenanthridines **10c,f** with decreased lipophicilities compared to diazacompounds (logD = 1.26 and 1.27), but to decreased binding affinities with *Ki* values of 39.4 and 4.84 nM respectively. With these results in hand, we investigated the SAR in the 7,10-diazaphenanthridine series. Therefore, insertion of substituents on **10g** was first evaluated in position 2, with fluorine (**10h**) and chlorine (**10i**) atoms leading to a strong decrease of binding affinities compared to **10g**. The introduction of a chlorine atom in position 3 (**10k**) led to the same result, whereas the fluorinated compound **10j** exhibited a higher binding affinity (*Ki* = 4.22 nM). We then explored the introduction of substituents in position 4. Insertion of bulky groups such as a trifluoromethyl (**10n**) or a methoxy (**10o**) led to decreased affinities. Introduction of a fluorine in position 4 (**10l**) led to a strongly decreased *Ki* value of 0.04 nM in guinea pig 5-HT_4Rs, whereas the chlorinated compound **10m** was found as potent as **10g**. When measured in human 5-HT_4Rs, **10l** and **10m** were found to exhibit higher affinities than **10g**, with very low *Ki* values of 0.029 and 0.026 nM respectively. LogD values were only slightly increased to 2.51 (**10l**) and 3.04 (**10m**) compared to 2.38 for **10g**. Based on these results, compound **14** with nitrogen atoms in position 7 and 10 and an iodine atom in position 4 was synthesized. Its binding affinity was found to be at 2.62 nM in guinea pig 5-HT_4Rs and 0.094 nM in human 5-HT_4Rs, while its measured logD value (logD = 3.47) was found to be more favourable for *in vivo* brain imaging studies compared against the parent compound **5** (logD = 4.28). The selectivity of **14** was then evaluated over a panel of 5-HTRs (Table 3). **14** exhibited a high selectivity over most of the 5-HTR (inhibition percentage < 50% at 10-6 M) and only a moderate affinity for the 5-$HT_{2a,b,c}$R subtypes (Ki = 20–130 nM) leading to a selectivity *ratio* above 500 for all tested 5-HTR, except for the 5-HT_{2C} receptor for which the selectivity *ratio* was lower, around 200. Moreover, compound **14** was found to be an antagonist with a K_B value of 0.18 nM (Table 3). Compared to [^{125}I]**5**, the insertion of an additional nitrogen atom in position 10 led to a decreased lipophilicity as expected, and also resulted in a slightly improved affinity. Therefore, **14** was radiolabeled with ^{125}I in a two-step sequence to afford [^{125}I]**14** (Scheme 3) and evaluated as a radiotracer. When injected in rat and followed *in vivo* by SPECT imaging (Fig. 1), compound [^{125}I]**14** showed its ability to cross the blood–brain barrier and to accumulate in brain tissue, with a preferential uptake in limbic regions known to

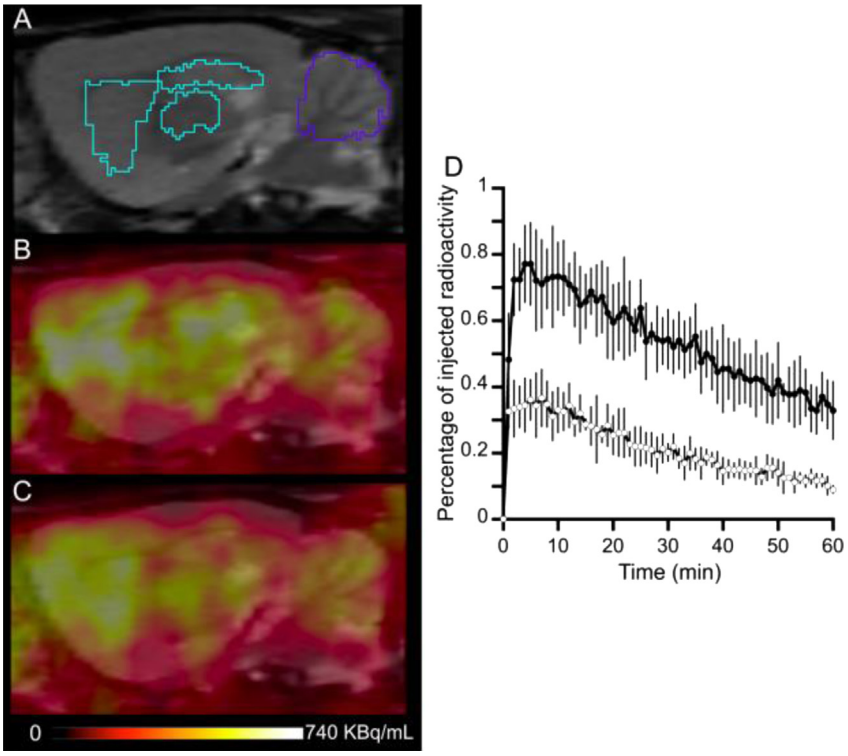

Fig. 1. *In vivo* SPECT imaging using compound [^{125}I]**14** in rat. Sectional views in the sagittal plane at corresponding anatomical levels of a reference MRI template (A) showing a part of limbic regions (outlined in light blue, made up of striatum, hippocampus and thalamus) and cerebellum (outlined in dark blue); and of representative SPECT scans averaged between 10 and 60 min post injection obtained with [^{125}I]**14** alone (B), or in the presence of **16** (C). Mean time–activity curves (±SD of 3 rats) observed in limbic regions (black) and cerebellum (white) obtained with [^{125}I]**14** (D). (For interpretation of the references to colour in this figure legend, the reader is referred to the web version of this article.)

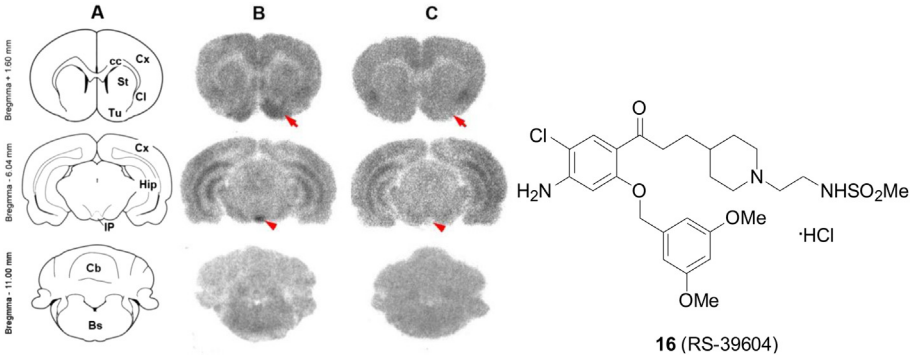

Fig. 2. *Ex vivo* competition between compound [^{125}I]**14** and the 5-HT$_4$R selective ligand **16**. Coronal sections of the rat brain: atlas outlines adapted from Paxinos and Watson [45] (A), *ex vivo* autoradiograms obtained with [^{125}I]**14** alone (B), or in presence of **16** (C). The inhibition of the binding of compound [^{125}I]**14** is visible in a few 5-HT$_4$R rich regions such as the olfactory tubercles (Tu, red arrows) or the interpeduncular nucleus (IP, red arrowheads). (Abbreviations: Bs, brainstem; Cb, cerebellum; cc, corpus callosum; Cl, claustrum; Cx, cortex; Hip, hippocampus; IP, interpeduncular nucleus; St, striatum; Tu, olfactory tubercles). (For interpretation of the references to colour in this figure legend, the reader is referred to the web version of this article.)

contain high densities of 5-HT$_4$R as compared to cerebellum, which is devoid of 5-HT$_4$R. In the SPECT experiment, the use of the 5-HT$_4$R selective antagonist **16** induces a visible decrease in the [^{125}I]**14** binding in 5-HT$_4$R rich region as compared to cerebellum. Ex vivo quantification of this effect showed a 54–56% reduction of radioactivity in the presence of **16** in some highly 5-HT$_4$R enriched regions [46] such as the interpeduncular nucleus (IP) or the brainstem (BS) (Fig. 2). However, only a lower displacement of [^{125}I]**14** binding occurred in other 5-HT$_4$R rich regions such as the hippocampal cornu ammonis fields (Hip). These results show that [^{125}I]**14** cannot be considered as a highly specific 5-HT$_4$R radiotracer. This hypothesis was further supported by the marked binding observed in the claustrum (Cl), a region not normally known for containing high densities of 5-HT$_4$R. The moderate affinity of **14** to 5-HT$_{2C}$R (Ki = 20 nM) could be part of this off-target signal especially in regions known to express significantly the 5-HT$_{2C}$ receptors (claustrum, olfactory tubercles, hippocampus) [45]. Nevertheless, binding of [^{125}I]**14** to other unknown brain targets, or lipophilic non-specific interactions cannot be excluded.

4. Conclusion

Starting from radioiodinated 5-HT$_4$R ligands **4**–**6** showing high unspecific binding and a homogeneous non-specific labelling of

Table 4
Quantification of autoradiographic data.[a]

Region	Specific binding ratio		Inhibition (%); *p value*
	[^{125}I]**14**	[^{125}I]**14** + **16**[b]	
IP	1.05 ± 0.17	0.45 ± 0.04	56.8; *p<0.01*
Hip	0.98 ± 0.10	0.72 ± 0.09	26.2; *p<0.05*
Cl	1.21 ± 0.16	0.77 ± 0.26	36.0; *p<0.05*
Tu	0.91 ± 0.22	0.55 ± 0.17	26.2; *p<0.05*
St	0.95 ± 0.15	0.56 ± 0.19	40.7; *p<0.05*
Bs	0.67 ± 0.22	0.30 ± 0.10	54.7; *p<0.05*
Cx	1.12 ± 0.01	0.69 ± 0.21	38.0; *p<0.05*

[a] Abbreviations: Bs, brainstem; Cl, claustrum; Cx, cortex; Hip, hippocampus; IP, interpeduncular nucleus; St, striatum; Tu, olfactory tubercles).
[b] 1 mg kg^{-1} of **16** was used. Data show mean ± SD of 3 rats. The *p* values were calculated using *t-test*.

brain tissues, we were able to design new 5-HT$_4$R ligands with improved lipophilicities and increased binding affinities. From these compounds, a radioiodinated ligand [^{125}I]**14** has been evaluated and has demonstrated its ability to specifically label some 5-HT$_4$R-containing regions. Nevertheless, the labelling of brain regions normally devoid of 5-HT$_4$R was still observed. This off-target labelling could either be due to a lipophilicity being still too high for a high specific binding, or to a lack of 5-HT$_4$R selectivity leading to a significant off-target binding. Despite this selectivity issue, our results demonstrated that slight structural modifications, and especially by decreasing the lipophilicity, strongly influence *in vivo* brain imaging and allows for a more specific signal to be obtained. These results encourage us to further explore this series to finally find a suitable brain 5-HT$_4$R radiotracer.

5. Experimental section

5.1. Chemistry

All chemical reagents and solvents were purchased from commercial sources and used without further purification except THF which was distilled from Na/benzophenone. Thin-layer chromatography (TLC) was performed on silica gel plates. Silica gel 0.06–0.20 mm was used for all column chromatography. Melting points were determined on a Kofler melting point apparatus. IR spectra were recorded on Perkin–Elmer IRFT 1650 spectrometer. ^{1}H (300 MHz) and ^{13}C (75 MHz) NMR spectra were recorded on a Bruker AvanceDMX 300 instrument with chemical shifts expressed in parts per million (in DMSO-d_6 or $CDCl_3$). High Resolution Mass Spectra (HRMS) were recorded with a Q-TOF Micromass Instrument in the positive ESI (CV = 30 V) mode. The purities of all tested compounds were analysed by LC-MS, with the purity all being higher than 95%. LC-MS Analyses were performed using a Waters alliance 2695 using the following gradient: A (95%)/B (5%) to A (5%)/B (95%) in 10 min. This ratio held for 3 min before return to initial conditions in 1 min. Initial conditions were then maintained for 5 min (A: H_2O, B: MeCN; each containing HCOOH: 0.1%; Column: C18 Xterra MSC118/2.1_50 mm). MS detection was performed with a Micromass ZMD 2000. All animal experiments were approved by the Swiss Cantonal Veterinary Office.

5.1.1. General procedure A for the synthesis of **7** and **8**

In a degassed solution of DME/water 2:1 (12 mL mmol^{-1} of diazine), was introduced *S*-Phos (10 mol%) and $Pd(OAc)_2$ (5 mol%). The solution was heated at 80 °C for 10 min and sodium carbonate (4 equiv), the arylboronic species (1.05 or 1.50 equiv) and 3-chloropyrazine-2-carbonitrile (1 equiv) were added. The solution was then refluxed (15 min or overnight) under argon. The resulting solution was filtrated on celite and washed with ethyl acetate and water. The aqueous phase was then extracted 3 times with ethyl acetate. The combined organic phases were washed with water, dried over $MgSO_4$ and evaporated to dryness. The residue was purified by silica gel chromatography to give the desired product.

*5.1.1.1. 2-Cyano-3-(2,5-difluorophenyl)pyrazine (**7**).* Starting from 2-chloro-3-cyanopyrazine (502 mg, 3.60 mmol) and 2,5-difluorophenylboronic acid [42] (855 mg, 5.41 mmol) following general procedure A, refluxing the reaction overnight and using PE/EtOAc (85:15) as eluent for the chromatography, **7** was obtained as a yellow solid (576 mg). Yield: 74%. Mp: 63–64 °C. IR (neat): ν (cm^{-1}) 3084, 2243, 1496, 1439, 1371, 1250, 1186. ^{1}H NMR (300 MHz, $CDCl_3$): δ 8.89 (d, J = 2.3 Hz, 1H), 8.74 (d, J = 2.3 Hz, 1H), 7.41–7.30 (m, 1H), 7.30–7.22 (m, 2H). ^{13}C NMR (75 MHz, $CDCl_3$): δ 158.6 (dd, ^1J = 245, ^4J = 2 Hz), 155.8 (dd, ^1J = 248, ^4J = 2 Hz), 152.2, 146.6, 143.9, 130.5, 124.0 (dd, ^2J = 17, ^3J = 8 Hz), 119.5 (dd, ^2J = 24, ^3J = 9 Hz), 117.8 (dd, ^2J = 25, ^3J = 7 Hz), 117.8 (dd, ^2J = 26, ^3J = 2 Hz), 114.9 (d, J = 1 Hz). HRMS/ESI: Calcd for $C_{11}H_5F_2N_3K$ [M+K]$^+$ 256.0089, found 256.0095.

*5.1.1.2. 2-Cyano-3-(5-chloro-2-fluorophenyl)pyrazine (**8**).* Starting from 2-chloro-3-cyanopyrazine (500 mg, 3.58 mmol) and 5-chloro-2-fluorophenylboronic acid [42] (666 mg, 3.76 mmol) following general procedure A, refluxing the reaction for 15 min and using PE/EtOAc (85:15) as eluent for the chromatography, **8** was obtained as a yellow solid (666 mg). Yield: 79%. Mp: 119–120 °C. IR (neat): ν (cm^{-1}) 2973, 2907, 2232, 1490, 1418, 1258, 1152, 1066. ^{1}H NMR (300 MHz, $CDCl_3$): δ 8.89 (d, J = 2.3 Hz, 1H), 8.74 (d, J = 2.3 Hz, 1H), 7.62 (dd, J = 6.1, 2.6 Hz, 1H), 7.53 (ddd, J = 8.8, 4.3, 2.6 Hz, 1H), 7.24 (dd, J = 9.5, 8.8 Hz, 1H). ^{13}C NMR (75 MHz, $CDCl_3$): 158.3 (d, ^1J = 252 Hz), 152.1 (d, ^3J = 1 Hz), 146.6, 144.0, 132.8 (d, ^3J = 9 Hz), 131.1 (d, ^3J = 2 Hz), 130.6 (d, ^4J = 1 Hz), 130.1 (d, ^4J = 3 Hz), 124.3 (d, ^2J = 16 Hz), 117.9 (d, ^2J = 23 Hz), 114.9 (d, J = 1 Hz). HRMS/ESI: Calcd for $C_{11}H_5ClFN_3Na$ [M+Na]$^+$ 256.0054, found 256.0050.

5.1.2. General procedure B for the synthesis of **9h** and **9i**

In a sealed tube were introduced **7** or **8** (1 equiv) and KOH (5 equiv) in *t*-BuOH (6 mL mmol^{-1} of **7** or **8**). The vial was sealed and the suspension was heated at 150 °C for 1.5 h. After cooling, the mixture was diluted with water, then an aqueous solution of HCl (2 M) was added until complete precipitation. The desired product was filtered, washed with water and dried *in vacuo*.

*5.1.2.1. 9-Fluoropyrazino[2,3-c]quinolin-5(6H)-one (**9h**).* Starting from **7** (455 mg, 2.10 mmol) and following general procedure B, **9h** was obtained as a yellow powder (384 mg). Yield: 85%. Mp: >260 °C. IR (neat): ν (cm^{-1}) 3505, 3038, 2902, 1684, 1507, 1461, 1256, 1200, 1177. ^{1}H NMR (300 MHz, DMSO-d_6): δ 12.15 (s, 1H), 9.11 (d, J = 2.1 Hz, 1H), 9.02 (d, J = 2.1 Hz, 1H), 8.23 (dd, J = 9.4, 2.8 Hz, 1H), 7.55 (ddd, J = 9.0, 8.6, 2.8 Hz, 1H), 7.45 (dd, J = 9.0, 4.8 Hz, 1H). ^{13}C NMR (75 MHz, DMSO-d_6): δ 159.2, 157.8 (d, ^1J = 239 Hz), 148.5, 146.0, 145.8 (d, ^4J = 3 Hz, 137.5, 134.5 (d, ^4J = 2 Hz), 119.8 (d, ^2J = 24 Hz), 119.0 (d, ^3J = 8 Hz), 118.0 (d, ^3J = 8 Hz), 109.3 (d, ^2J = 24 Hz). HRMS/ESI: Calcd for $C_{11}H_7FN_3O$ [M+H]$^+$ 216.0573, found 216.0574.

*5.1.2.2. 9-Chloropyrazino[2,3-c]quinolin-5(6H)-one (**9i**).* Starting from **8** (499 mg, 2.14 mmol) and following general procedure B, **9i** was obtained as a yellow powder (460 mg). Yield: 93%. Mp: >260 °C. IR (neat): ν (cm^{-1}) 3483, 3036, 2888, 1679, 1450, 1351, 1253, 1195, 1118. ^{1}H NMR (300 MHz, DMSO-d_6): δ 12.20 (s, 1H), 9.11 (d, J = 1.8 Hz, 1H), 9.01 (d, J = 1.8 Hz, 1H), 8.47 (d, J = 2.0 Hz, 1H), 7.69 (dd, J = 8.7, 2.2 Hz, 1H), 7.43 (d, J = 8.7 Hz, 1H). ^{13}C NMR (75 MHz, DMSO-d_6): δ 159.4, 148.6, 146.0, 145.5, 137.4, 136.6, 131.8, 126.8, 123.2, 119.3, 118.0. HRMS/ESI: Calcd for $C_{11}H_6ClN_3ONa$ [M+Na]$^+$ 254.0097, found 254.0095.

5.1.3. General procedure C for the synthesis of 10a–o and 14

Oxalyl chloride (10.3 equiv) and DMF (10.7 equiv) were added to chloroform (1 mL per 0.15 mmol of **9a**–**o** or **13**) at 0 °C and the solution was stirred during 3 h at room temperature. **9a**–**o** or **13** (1 equiv) was then added in one time to the mixture and the solution was refluxed for 2 h. The resulting mixture was carefully hydrolysed with water and the pH was adjusted to 10 using an aqueous ammonia solution (28%). The resulting solution was extracted with dichloromethane, dried with $MgSO_4$, filtrated, evaporated and quickly eluted on a pad of silica gel using PE/EtOAc as eluent to afford the expected pure chlorimine derivatives. In a Schlenk flask, LHMDS (1.1 equiv) was added to a solution of 1-propylpiperidin-4-ylmethanol (1.05 equiv) in dry DMF (10 mL $mmol^{-1}$ of **9a**–**o** or **13**) under N_2 at 0 °C. The reaction mixture was stirred for 15 min and warmed to room temperature for 15 min. The selected chlorimine obtained above, was diluted in dry DMF (10 mL $mmol^{-1}$ of **9a**–**o** or **13**) and added neat *via* syringe in the Schlenk. The reaction mixture was stirred at room temperature overnight. Cold water was then added and the resulting mixture was extracted with ethyl acetate, dried with $MgSO_4$, filtrated and evaporated. The crude product was then purified by silica gel chromatography using PE/EtOAc +2% of Et_3N as eluent to obtain the desired compound **10a**–**o** or **14**.

*5.1.3.1. 6-(1-Propylpiperidin-4-yl)methyloxypyrimido[5,4-c]isoquinoline (**10a**).* 5-Amino-4-chloropyrimidine (51 mg, 0.39 mmol) and ethyl 2-(5,5-dimethyl-1,3,2-dioxaborinan-2-yl)benzoate [42] (306 mg, 1.17 mmol) were dissolved in a mixture of dioxane/water 12:1 (3 mL), then K_3PO_4 (248 mg, 1.17 mmol) and $Pd(PPh_3)_4$ (36 mg, 8 mol%) were added. The reaction mixture was refluxed overnight, cooled to room temperature and evaporated to dryness. The resulting crude diazaphenanthridinone **9a** was then reacted following general procedure C. **10a** (28 mg) was obtained as a yellow powder. R_f (petroleum ether/EtOAc (50:50)) = 0.21. Yield: 21% (over three steps). Mp: 110–111 °C. IR (neat): ν (cm^{-1}) 2958, 2914, 1575, 1454, 1393, 1336, 1314, 1146, 1088. ^{1}H NMR (300 MHz, $CDCl_3$): δ 9.27 (s, 1H), 9.25 (s, 1H), 9.02 (d, J = 7.8 Hz, 1H), 8.37 (d, J = 7.8 Hz, 1H), 7.93 (ddd, J = J = 7.8 Hz, J = 1.2 Hz, 1H), 7.85 (ddd, J = J = 7.8 Hz, J = 1.2 Hz, 1H), 4.51 (d, J = 6.1 Hz, 2H), 3.04 (d, J = 11.4 Hz, 2H), 2.36–2.30 (m, 2H), 2.12–1.84 (m, 5H), 1.72–1.45 (m, 4H), 0.90 (t, J = 7.4 Hz, 3H). ^{13}C NMR (75 MHz, $CDCl_3$): δ 160.1, 156.8, 153.6, 144.7, 135.5, 133.7, 131.9, 131.0, 124.7, 123.8, 123.7, 71.3, 61.1, 53.5 (2C), 35.7, 29.1 (2C), 20.1, 12.0. LC–MS (ESI): t_R = 4.71 min; $[M+H]^+$ 337.43. HRMS/ESI: Calcd for $C_{20}H_{25}N_4O$ $[M+H]^+$ 337.2028, found 337.2027.

*5.1.3.2. 6-(1-Propylpiperidin-4-yl)methyloxypyrazino[2,3-c]isoquinoline (**10b**).* 2-Amino-3-chloropyrazine (156 mg, 1.20 mmol) and ethyl 2-(5,5-dimethyl-1,3,2-dioxaborinan-2-yl)benzoate [42] (306 mg, 3.60 mmol) were dissolved in a mixture of dioxane/water 12:1 (9.2 mL), then K_3PO_4 (764 mg, 3.60 mmol) and $Pd(PPh_3)_4$ (111 mg, 8 mol%) were added. The reaction mixture was refluxed overnight, cooled to room temperature and evaporated to dryness. The resulting crude diazaphenanthridinone **9b** was then reacted following general procedure C. **10b** (178 mg) was obtained as a yellow powder. Yield: 44% (over three steps). R_f ($EtOAc/Et_3N$ (98:2)) = 0.20. Mp: 110–111 °C. IR (neat): ν (cm^{-1}) 2924, 1593, 1455, 1374, 1338, 1312, 1300, 1165, 1092, 982. ^{1}H NMR (300 MHz, $CDCl_3$): δ 9.02 (d, J = 7.8 Hz, 1H), 8.82 (d, J = 2.1 Hz, 1H), 8.74 (d, J = 2.1 Hz, 1H), 8.39 (d, J = 7.8 Hz, 1H), 7.93 (ddd, J = J = 7.8 Hz, J = 1.1 Hz, 1H), 7.80 (ddd, J = J = 7.8 Hz, J = 1.1 Hz, 1H), 4.63 (d, J = 6.3 Hz, 2H), 3.03 (d, J = 11.5 Hz, 2H), 2.34–2.29 (m, 2H), 2.09–1.89 (m, 5H), 1.69–1.46 (m, 4H), 0.91 (t, J = 7.3 Hz, 3H). ^{13}C NMR (75 MHz, $CDCl_3$): δ 162.0, 148.7, 145.0, 141.2, 135.5, 135.1, 131.9, 129.8, 124.8, 123.8, 122.3, 71.8, 61.1, 53.4 (2C), 35.6, 29.1 (2C), 20.1, 12.0. LC–MS (ESI): t_R = 4.75 min; $[M+Na]^+$ 359.52. HRMS/ESI: Calcd for $C_{20}H_{25}N_4O$ $[M+H]^+$ 337.2028, found 337.2016.

*5.1.3.3. 6-(1-Propylpiperidin-4-yl)methyloxypyrazino[2,3-c][2,6]naphthyridine (**10c**).* Starting from **9c** (146 mg, 0.74 mmol) using general procedure C, **10c** (26 mg) was obtained as a yellow powder. Yield: 10%. R_f ($EtOAc/Et_3N$ (98:2)) = 0.10. Mp: 126–127 °C. IR (neat): ν (cm^{-1}) 2932, 2774, 1591, 1398, 1377, 1334, 1313, 983. ^{1}H NMR (300 MHz, $CDCl_3$): δ 10.33 (d, J = 0.8 Hz, 1H), 9.00 (d, J = 5.5 Hz, 1H), 8.87 (d, J = 2.1 Hz, 1H), 8.80 (d, J = 2.1 Hz, 1H), 8.12 (dd, J = 5.5, J = 0.8 Hz, 1H), 4.62 (d, J = 6.4 Hz, 2H), 3.00 (d, J = 11.5 Hz, 2H), 2.39–2.24 (m, 2H), 2.07–1.84 (m, 5H), 1.65–1.42 (m, 4H), 0.89 (t, J = 7.4 Hz, 3H). ^{13}C NMR (75 MHz, $CDCl_3$): δ 161.1, 149.2, 148.7, 148.3, 145.8, 142.3, 134.1, 128.6, 126.5, 116.9, 72.4, 61.1, 53.4 (2C), 35.5, 29.1 (2C), 20.1, 12.0. LC–MS (ESI): t_R = 4.09 min; $[M+H]^+$ 338.43. HRMS/ESI: Calcd for $C_{19}H_{24}N_5O$ $[M+H]^+$ 338.1981, found 338.1989.

*5.1.3.4. 6-(1-Propylpiperidin-4-yl)methyloxypyrimido[4,5-c]isoquinoline (**10d**).* Starting from **9d** (73 mg, 0.37 mmol) using general procedure C, **10d** (40 mg) was obtained as a yellow powder. Yield: 32%. R_f ($EtOAc/Et_3N$ (98:2)) = 0.30. Mp: 126–127 °C. IR (neat): ν (cm^{-1}) 2936, 2765, 1585, 1560, 1406, 1340, 1310, 1269. ^{1}H NMR (300 MHz, $CDCl_3$): δ 9.79 (s, 1H), 9.34 (s, 1H), 8.55 (d, J = 8.0 Hz, 1H), 8.45 (d, J = 8.0 Hz, 1H), 7.93 (ddd, J = J = 8.0 Hz, J = 1.1 Hz, 1H), 7.76 (dd, J = J = 8.0 Hz, 1H), 4.65 (d, J = 6.3 Hz, 2H), 3.01 (d, J = 11.6 Hz, 2H), 2.36–2.26 (m, 2H), 2.10–1.82 (m, 5H), 1.66–1.43 (m, 4H), 0.90 (t, J = 7.4 Hz, 3H). ^{13}C NMR (75 MHz, $CDCl_3$): δ 165.4, 158.4, 157.9, 153.6, 132.9, 132.6, 129.1, 125.8, 121.4, 120.7, 114.7, 72.3, 61.2, 53.5 (2C), 35.6, 29.1 (2C), 20.2, 12.1. LC–MS (ESI): t_R = 4.36 min; $[M+H]^+$ 337.47. HRMS/ESI: Calcd for $C_{20}H_{25}N_4O$ $[M+H]^+$ 337.2028, found 337.2022.

*5.1.3.5. 6-(1-Propylpiperidin-4-yl)methyloxypyridazino[3,4-c]isoquinoline (**10e**).* *S*-Phos (22 mg, 10 mol%) was introduced in dry toluene (1 mL) under argon, then $Pd(OAc)_2$ (6 mg, 5 mol%) was added. The resulting solution was heated at 80 °C for 10 min. A solution of *N*-(4-(tri(*n*-butyl)stannyl)pyridazin-3-yl)pivalamide [42] (260 mg, 0.54 mmol) in dry toluene (1.6 mL) and ethyl 2-iodobenzoate (120 μL, 0.80 mmol) were successively added. The solution was refluxed overnight and the resulting mixture was evaporated to dryness. The resulting crude diazaphenanthridinone **9e** was then reacted following general procedure C. **10e** (80 mg) was obtained as a yellow powder. Yield: 42% (over three steps). R_f ($EtOAc/Et_3N$ (98:2)) = 0.06. Mp: 173–174 °C. IR (neat): ν (cm^{-1}) 2938, 2771, 1592, 1455, 1329, 1268, 1244, 1093, 982. ^{1}H NMR (300 MHz, $CDCl_3$): δ 9.34 (d, J = 5.4 Hz, 1H), 8.53 (d, J = 7.9 Hz, 1H), 8.47 (d, J = 7.3 Hz, 1H), 8.33 (d, J = 5.4 Hz, 1H), 7.93 (dd, J = 7.9, 7.5 Hz, 1H), 7.85 (dd, J = 7.5, 7.3 Hz, 1H), 4.70 (d, J = 6.2 Hz, 2H), 3.09 (d, J = 11.3 Hz, 2H), 2.46–2.33 (m, 2H), 2.15–1.92 (m, 5H), 1.79–1.52 (m, 4H), 0.91 (t, J = 7.4 Hz, 3H). ^{13}C NMR (75 MHz, $CDCl_3$): δ 162.7, 156.3, 146.8, 132.2, 132.1, 130.8, 125.8, 123.2, 122.2, 119.1, 118.9, 71.8, 60.8, 53.3 (2C), 35.3, 28.7 (2C), 19.8, 11.9. LC–MS (ESI): t_R = 4.30 min; $[M+H]^+$ 337.39. HRMS/ESI: Calcd for $C_{20}H_{25}N_4O$ $[M+H]^+$ 337.2028, found 337.2038.

*5.1.3.6. 5-(1-Propylpiperidin-4-yl)methyloxypyrazino[2,3-c][1,8]naphthyridine (**10f**).* Starting from **9f** (49 mg, 0.25 mmol) using general procedure C, **10f** (42 mg) was obtained as a yellow powder. Yield: 50%. R_f ($EtOAc/Et_3N$ (98:2)) = 0.12. Mp: 138–139 °C. IR (neat): ν (cm^{-1}) 2934, 2760, 1595, 1575, 1455, 1345, 1315, 1190, 1133. ^{1}H NMR (300 MHz, $CDCl_3$): δ 9.19 (dd, J = 8.0, 2.2 Hz, 1H), 9.08 (d, J = 2.0 Hz, 1H), 9.03 (d, J = 2.0 Hz, 1H), 9.01 (dd, J = 4.7, 2.2 Hz, 1H), 7.53 (dd, J = 8.0, 4.7 Hz, 1H), 4.68 (d, J = 7.0 Hz, 2H), 2.97 (d, J = 11.3 Hz, 2H), 2.37–2.21 (m, 2H), 2.21–2.04 (m, 1H), 1.99–1.92 (m, 4H), 1.59–1.40 (m, 4H), 0.87 (t, J = 7.4 Hz, 3H). ^{13}C NMR

(75 MHz, $CDCl_3$): δ 160.9, 154.2, 153.3, 148.0, 145.5, 145.5, 133.4, 131.2, 120.9, 117.6, 72.7, 61.1, 53.3 (2C), 35.1, 29.1 (2C), 20.1, 12.0. LC–MS (ESI): t_R = 3.73 min; $[M+H]^+$ 338.44. HRMS/ESI: Calcd for $C_{19}H_{24}N_5O$: $[M+H]^+$ 338.1981, found 338.1971.

*5.1.3.7. 5-(1-Propylpiperidin-4-yl)methyloxypyrazino[2,3-c]quinoline (**10g**).* Starting from **9g** (71 mg, 0.36 mmol) using general procedure C, **10g** (74 mg) was obtained as a white powder. Yield: 61%. R_f (EtOAc/Et_3N (98:2)) = 0.19. Mp: 137–138 °C. IR (neat): ν (cm^{-1}) 2956, 2930, 2777, 1592, 1458, 1439, 1350, 1329, 1194, 1136, 1107, 1054. ^1H NMR (300 MHz, $CDCl_3$): δ 9.04 (d, J = 2.0 Hz, 1H), 8.96 (d, J = 2.0 Hz, 1H), 8.87 (dd, J = 8.1, 1.3 Hz, 1H), 7.89 (d, J = 8.1 Hz, 1H), 7.75 (ddd, J = 8.1, 7.0, 1.3 Hz, 1H), 7.56 (ddd, J = 8.1, 7.0, 1.3 Hz, 1H), 4.58 (d, J = 6.9 Hz, 2H), 2.98 (d, J = 11.3 Hz, 2H), 2.34–2.22 (m, 2H), 2.20–2.04 (m, 1H), 2.00–1.96 (m, 4H), 1.62–1.42 (m, 4H), 0.89 (t, J = 7.4 Hz, 3H). ^{13}C NMR (75 MHz, $CDCl_3$): δ 158.0, 147.4, 145.8, 144.7, 144.4, 131.3, 131.1, 127.3, 125.2, 123.9, 122.6, 71.7, 61.2, 53.5 (2C), 35.4, 29.3 (2C), 20.2, 12.1. LC–MS (ESI): t_R = 4.84 min; $[M+H]^+$ 337.41. HRMS/ESI: Calcd for $C_{20}H_{25}N_4O$ $[M+H]^+$ 337.2028, found 337.2033.

*5.1.3.8. 9-Fluoro-5-(1-propylpiperidin-4-yl)methyloxypyrazino[2,3-c]quinoline (**10h**).* Starting from **9h** (122 mg, 0.57 mmol) using general procedure C, **10h** (135 mg) was obtained as a yellow powder. Yield: 67%. R_f (EtOAc/Et_3N (98:2)) = 0.22. Mp: 153–154 °C. IR (neat): ν (cm^{-1}) 2923, 1593, 1470, 1331, 1210, 1134, 1102, 1049. ^1H NMR (300 MHz, $CDCl_3$): δ 9.05 (d, J = 2.0 Hz, 1H), 9.01 (d, J = 2.0 Hz, 1H), 8.50 (dd, J = 9.2, 3.0 Hz, 1H), 7.88 (dd, J = 8.9, 5.1 Hz, 1H), 7.48 (ddd, J = 8.9, 8.3, 3.0 Hz, 1H), 4.57 (d, J = 6.9 Hz, 2H), 3.00 (d, J = 11.7 Hz, 2H), 2.37–2.25 (m, 2H), 2.18–2.05 (m, 1H), 2.02–1.94 (m, 4H), 1.62–1.44 (m, 4H), 0.90 (t, J = 7.4 Hz, 3H). ^{13}C NMR (75 MHz, $CDCl_3$): δ 160.2 (d, ^1J = 245 Hz), 157.6, 147.4, 145.3 (d, ^4J = 4 Hz), 145.3, 141.0 (d, ^4J = 2 Hz), 131.3, 129.3 (d, ^3J = 9 Hz), 123.9 (d, ^3J = 9 Hz), 119.9 (d, ^2J = 24 Hz), 108.9 (d, ^2J = 24 Hz), 71.8, 61.2, 53.5 (2C), 35.4, 29.2 (2C), 20.2, 12.1. LC–MS (ESI): t_R = 4.91 min; $[M+H]^+$ 355.38. HRMS/ESI: Calcd for $C_{20}H_{24}FN_4O$ $[M+H]^+$ 355.1934, found 355.1935.

*5.1.3.9. 9-Chloro-5-(1-propylpiperidin-4-yl)methyloxypyrazino[2,3-c]quinoline (**10i**).* Starting from **9i** (128 mg, 0.55 mmol) using general procedure C, **10i** (117 mg) was obtained as a yellow powder. Yield: 57%. R_f (EtOAc/Et_3N (98:2)) = 0.19. Mp: 155–156 °C. IR (neat): ν (cm^{-1}) 2931, 1591, 1450, 1330, 1199, 1138, 1053. ^1H NMR (300 MHz, $CDCl_3$): δ 9.06 (d, J = 2.0 Hz, 1H), 9.00 (d, J = 2.0 Hz, 1H), 8.84 (d, J = 2.4 Hz, 1H), 7.83 (d, J = 8.7 Hz, 1H), 7.69 (dd, J = 8.7, 2.4 Hz, 1H), 4.57 (d, J = 6.9 Hz, 2H), 3.00 (d, J = 11.7 Hz, 2H), 2.35–2.26 (m, 2H), 2.19–2.05 (m, 1H), 2.04–1.94 (m, 4H), 1.64–1.44 (m, 4H), 0.90 (t, J = 7.4 Hz, 3H). ^{13}C NMR (75 MHz, $CDCl_3$): δ 158.3, 147.6, 145.3, 145.0, 142.8, 131.7, 131.3, 131.1, 128.8, 123.7, 123.4, 71.9, 61.2, 53.5 (2C), 35.4, 29.2 (2C), 20.2, 12.1. LC–MS (ESI): t_R = 5.31 min; $[M+H]^+$ 371.39, 373.40. HRMS/ESI: Calcd for $C_{20}H_{24}ClN_4O$ $[M+H]^+$ 371.1639, found 371.1632.

*5.1.3.10. 8-Fluoro-5-(1-propylpiperidin-4-yl)methyloxypyrazino[2,3-c]quinoline (**10j**).* Starting from **9j** (84 mg, 0.39 mmol) using general procedure C, **10j** (93 mg) was obtained as a yellow powder. Yield: 67%. R_f (EtOAc/Et_3N (98:2)) = 0.25. Mp: 143–144 °C. IR (neat): ν (cm^{-1}) 2942, 2772, 1587, 1481, 1333, 1277, 1189, 1132, 1053. ^1H NMR (300 MHz, $CDCl_3$): δ 8.97 (d, J = 2.0 Hz, 1H), 8.89 (d, J = 2.0 Hz, 1H), 8.79 (dd, J = 8.8, 6.4 Hz, 1H), 7.48 (dd, J = 10.0, 2.6 Hz, 1H), 7.24 (ddd, J = 8.8, 8.2, 2.6 Hz, 1H), 4.51 (d, J = 6.9 Hz, 2H), 2.93 (d, J = 11.6 Hz, 2H), 2.29–2.18 (m, 2H), 2.13–1.98 (m, 1H), 1.98–1.84 (m, 4H), 1.54–1.36 (m, 4H), 0.83 (t, J = 7.4 Hz, 3H). ^{13}C NMR (75 MHz, $CDCl_3$): δ 164.7 (d, ^1J = 250 Hz), 159.0, 147.6, 146.0 (d, ^3J = 13 Hz), 145.6, 144.6, 130.7, 126.1 (d, ^3J = 10 Hz), 119.3 (d, ^4J = 2 Hz), 114.1 (d, ^2J = 24 Hz), 112.5 (d, ^2J = 22 Hz), 72.0, 61.2, 53.5 (2C), 35.4, 29.2 (2C), 20.2, 12.1. LC–MS (ESI): t_R = 4.99 min; $[M+H]^+$ 355.41. HRMS/ESI: Calcd for $C_{20}H_{24}FN_4O$ $[M+H]^+$ 355.1934, found 355.1942.

*5.1.3.11. 8-Chloro-5-(1-propylpiperidin-4-yl)methyloxypyrazino[2,3-c]quinoline (**10k**).* Starting from **9k** (93 mg, 0.40 mmol) using general procedure C, **10k** (79 mg) was obtained as a yellow powder. Yield: 53%. R_f (EtOAc/Et_3N (98:2)) = 0.17. Mp: 125–126 °C. IR (neat): ν (cm^{-1}) 2942, 2874, 2772, 1592, 1457, 1435, 1328, 1197, 1114. ^1H NMR (300 MHz, $CDCl_3$): δ 9.02 (d, J = 2.0 Hz, 1H), 8.96 (d, J = 2.0 Hz, 1H), 8.76 (d, J = 8.6 Hz, 1H), 7.87 (d, J = 2.0 Hz, 1H), 7.50 (dd, J = 8.6, 2.0 Hz, 1H), 4.55 (d, J = 6.9 Hz, 2H), 2.98 (d, J = 11.7 Hz, 2H), 2.33–2.24 (m, 2H), 2.19–2.04 (m, 1H), 2.04–1.88 (m, 4H), 1.62–1.41 (m, 4H), 0.88 (t, J = 7.4 Hz, 3H). ^{13}C NMR (75 MHz, $CDCl_3$): δ 158.9, 147.6, 145.4, 145.1, 144.9, 137.2, 131.0, 126.7, 125.8, 125.2, 121.1, 72.0, 61.1, 53.4 (2C), 35.3, 29.2 (2C), 20.2, 12.1. LC–MS (ESI): t_R = 5.31 min; $[M+H]^+$ 371.37, 373.38. HRMS/ESI: Calcd for $C_{20}H_{24}ClN_4O$ $[M+H]^+$ 371.1639, found 371.1645.

*5.1.3.12. 7-Fluoro-5-(1-propylpiperidin-4-yl)methyloxypyrazino[2,3-c]quinoline (**10l**).* Starting from **9l** (98 mg, 0.45 mmol) using general procedure C, **10l** (130 mg) was obtained as a yellow powder. Yield: 80%. R_f (EtOAc/Et_3N (98:2)) = 0.25. Mp: 148–149 °C. IR (neat): ν (cm^{-1}) 2945, 2773, 1593, 1432, 1355, 1330, 1237, 1085. ^1H NMR (300 MHz, $CDCl_3$): δ 9.08 (d, J = 2.0 Hz, 1H), 9.02 (d, J = 2.0 Hz, 1H), 8.67 (dd, J = 6.5, 2.9 Hz, 1H), 7.52–7.48 (m, 2H), 4.65 (d, J = 6.9 Hz, 2H), 3.00 (d, J = 11.6 Hz, 2H), 2.43–2.22 (m, 2H), 2.19–2.07 (m, 1H), 2.04–1.95 (m, 4H), 1.59–1.47 (m, 4H), 0.90 (t, J = 7.4 Hz, 3H). ^{13}C NMR (75 MHz, $CDCl_3$): δ 158.2, 156.8 (d, ^1J = 253 Hz), 147.6, 145.4 (d, J = 4 Hz), 145.2, 133.6 (d, ^2J = 11 Hz), 131.3, 125.1 (d, ^3J = 8 Hz), 124.7 (d, J = 2 Hz), 119.4 (d, ^4J = 4 Hz), 116.5 (d, ^2J = 19 Hz), 72.0, 61.2, 53.5 (2C), 35.5, 29.2 (2C), 20.2, 12.0. LC–MS (ESI): t_R = 4.81 min; $[M+H]^+$ 355.38. HRMS/ESI: Calcd for $C_{20}H_{24}FN_4O$ $[M+H]^+$ 355.1934, found 355.1930.

*5.1.3.13. 7-Chloro-5-(1-propylpiperidin-4-yl)methyloxypyrazino[2,3-c]quinoline (**10m**).* Starting from **9m** (77 mg, 0.33 mmol) using general procedure C, **10m** (95 mg) was obtained as a yellow powder. Yield: 77%. R_f (EtOAc/Et_3N (98:2)) = 0.17. Mp: 139–140 °C. IR (neat): ν (cm^{-1}) 2971, 2939, 2766, 1592, 1456, 1429, 1351, 1178, 1121, 1051, 974. ^1H NMR (300 MHz, $CDCl_3$): δ 9.08 (d, J = 2.0 Hz, 1H), 9.01 (d, J = 2.0 Hz, 1H), 8.82 (dd, J = 8.1, 1.3 Hz, 1H), 7.87 (dd, J = 7.7, 1.3 Hz, 1H), 7.49 (dd, J = 8.1, 7.7 Hz, 1H), 4.70 (d, J = 6.8 Hz, 2H), 2.99 (d, J = 11.4 Hz, 2H), 2.32–2.27 (m, 2H), 2.24–2.10 (m, 1H), 2.04–1.94 (m, 4H), 1.62–1.42 (m, 4H), 0.89 (t, J = 7.4 Hz, 3H). ^{13}C NMR (75 MHz, $CDCl_3$): δ 158.3, 147.7, 145.7, 145.3, 140.7, 131.7, 131.6, 131.1, 125.2, 124.3, 122.8, 72.2, 61.2, 53.5 (2C), 35.5, 29.3 (2C), 20.2, 12.1. LC–MS (ESI): t_R = 5.17 min; $[M+H]^+$ 371.39, 373.40. HRMS/ESI: Calcd for $C_{20}H_{24}ClN_4O$ $[M+H]^+$ 371.1639, found 371.1631.

*5.1.3.14. 7-Trifluoromethyl-5-(1-propylpiperidin-4-yl)methyloxypyrazino[2,3-c]quinoline (**10n**).* Starting from **9n** (124 mg, 0.46 mmol) using general procedure C, **10n** (134 mg) was obtained as a yellow powder. Yield: 71%. R_f (EtOAc/Et_3N (98:2)) = 0.27. Mp: 139–140 °C. IR (neat): ν (cm^{-1}) 2935, 2768, 1592, 1476, 1437, 1339, 1301, 1133, 1052, 1029. ^1H NMR (300 MHz, $CDCl_3$): δ 9.09 (d, J = 1.9 Hz, 1H), 9.08 (m, 1H), 9.03 (d, J = 1.9 Hz, 1H), 8.09 (d, J = 7.6 Hz, 1H), 7.61 (dd, J = J = 7.6 Hz, 1H), 4.67 (d, J = 6.8 Hz, 2H), 2.97 (d, J = 11.2 Hz, 2H), 2.31–2.23 (m, 2H), 2.24–2.08 (m, 1H), 1.97–1.90 (m, 4H), 1.60–1.41 (m, 4H), 0.88 (t, J = 7.4 Hz, 3H). ^{13}C NMR (75 MHz, $CDCl_3$): δ 158.1, 147.8, 145.5, 145.3, 141.4, 130.9, 129.1 (q, ^3J = 5 Hz), 128.0, 126.4 (q, ^2J = 30 Hz), 124.1, 124.0 (q, ^1J = 273 Hz), 123.6, 72.5, 61.1, 53.5 (2C), 35.1, 29.1 (2C), 20.2, 12.1. LC–MS (ESI): t_R = 5.34 min; $[M+H]^+$ 405.39. HRMS/ESI: Calcd for $C_{21}H_{24}F_3N_4O$ $[M+H]^+$ 405.1902, found 405.1907.

*5.1.3.15. 7-Methoxy-5-(1-propylpiperidin-4-yl)methyloxypyrazino [2,3-c]quinoline (**10o**).* Starting from **9o** (78 mg, 0.34 mmol) using general procedure C, **10o** (58 mg) was obtained as a yellow powder. Yield: 46%. R_f (EtOAc/Et_3N (98:2)) = 0.15. Mp: 140–141 °C. IR (neat): ν (cm^{-1}) 2927, 2811, 1590, 1332, 1260, 1239, 1100, 1048. ^1H NMR (300 MHz, $CDCl_3$): δ 9.06 (d, J = 2.0 Hz, 1H), 8.99 (d, J = 2.0 Hz, 1H), 8.50 (dd, J = 8.1, 1.2 Hz, 1H), 7.53 (dd, $J = J$ = 8.1 Hz, 1H), 7.24 (m, 1H), 4.64 (d, J = 6.9 Hz, 2H), 4.09 (s, 3H), 3.00 (d, J = 11.2 Hz, 2H), 2.34–2.26 (m, 2H), 2.18–2.06 (m, 1H), 2.05–1.92 (m, 4H), 1.64–1.45 (m, 4H), 0.90 (t, J = 7.4 Hz, 3H). ^{13}C NMR (75 MHz, $CDCl_3$): δ 157.5, 154.1, 147.5, 145.9, 145.0, 134.9, 131.1, 125.5, 124.0, 115.9, 111.8, 71.6, 61.2, 56.5, 53.5 (2C), 35.6, 29.2 (2C), 20.2, 12.1. LC–MS (ESI): t_R = 4.57 min; $[M+H]^+$ 367.40. HRMS/ESI: Calcd for $C_{21}H_{27}N_4O_2$ $[M+H]^+$ 367.2134, found 367.2131.

*5.1.3.16. 2-Cyano-3-(2-fluoro-3-trimethylsilylphenyl)pyrazine (**11**).* Starting from 2-chloro-3-cyanopyrazine (1.00 g, 7.17 mmol) and 2-fluoro-3-trimethylsilylphenylboronic acid [33] (1.60 g, 7.52 mmol) following general procedure A, refluxing the reaction 15 min and using PE/EtOAc (9:1) as eluent for the column chromatography, **11** (1.74 g) was obtained as a yellow oil. Yield: 90%. IR (neat): ν (cm^{-1}) 2958, 2242, 1605, 1409, 1392, 1250, 1203, 1143, 1073, 1040. ^1H NMR (300 MHz, $CDCl_3$): δ 8.87 (d, J = 2.3 Hz, 1H), 8.69 (d, J = 2.3 Hz, 1H), 7.64–7.59 (m, 2H), 7.33 (dd, $J = J$ = 7.4 Hz, 1H), 0.38 (s, 9H). ^{13}C NMR (75 MHz, $CDCl_3$): δ 164.0 (d, ^1J = 246 Hz), 154.2 (d, ^3J = 1 Hz), 146.4, 143.3, 138.2 (d, ^3J = 12 Hz), 132.5 (d, ^3J = 2 Hz), 130.8 (d, ^4J = 1 Hz), 127.9 (d, ^2J = 32 Hz), 124.5 (d, ^4J = 3 Hz), 122.2 (d, ^2J = 18 Hz), 115.3 (d, ^5J = 1 Hz), −1.1 (d, ^4J = 2 Hz, 3C). HRMS/ESI: Calcd for $C_{14}H_{14}FN_3SiNa$ $[M+Na]^+$ 294.0839, found 294.0844.

*5.1.4. 2-Cyano-3-(2-fluoro-3-iodophenyl)pyrazine (**12**)*

In a round-bottom flask were introduced **11** (93 mg, 0.34 mmol), DCM (2.8 mL) and ICl (86 mg, 0.53 mmol). The solution was stirred for 4.5 h at room temperature and a saturated aqueous $Na_2S_2O_3$ solution (2 mL) was added. The aqueous layer was then extracted with DCM (3 x 10 mL) and the combined organic layers were dried over $MgSO_4$, filtered and evaporated *in vacuo*. The crude was purified by silica gel chromatography (eluent: PE/EtOAc (9:1)) to give **12** (84 mg) as a white powder. Yield: 76%. Mp: 132–133 °C. IR (neat): ν (cm^{-1}) 2925, 2849, 2244, 1598, 1530, 1430, 1386, 1232, 1138. ^1H NMR (300 MHz, $CDCl_3$): δ 8.88 (d, J = 2.3 Hz, 1H), 8.74 (d, J = 2.3 Hz, 1H), 7.97 (ddd, J = 7.7, 6.3, 1.6 Hz, 1H), 7.59 (ddd, J = 7.7, 6.3, 1.6 Hz, 1H), 7.12 (dd, $J = J$ = 7.7 Hz, 1H). ^{13}C NMR (75 MHz, $CDCl_3$): δ 158.7 (d, ^1J = 250 Hz), 152.9 (d, ^3J = 2 Hz), 146.5, 143.9, 142.3 (d, ^3J = 2 Hz), 131.5 (d, ^3J = 2 Hz), 130.5 (d, ^4J = 1 Hz), 126.2 (d, ^4J = 4 Hz), 123.5 (d, ^2J = 16 Hz), 115.0 (d, ^5J = 1 Hz), 82.4 (d, ^2J = 26 Hz). HRMS/ESI: Calcd for $C_{11}H_5FIN_3Na$ $[M+Na]^+$ 347.9410, found 347.9417.

*5.1.5. 7-Iodopyrazino[2,3-c]quinolin-5(6H)-one (**13**)*

Starting from **12** (63 mg, 0.19 mmol) and following general procedure B, **13** (46 mg) was obtained as a yellow powder. Yield: 73%. Mp: >260 °C. IR (neat): ν (cm^{-1}) 3328, 2913, 1680, 1483, 1431, 1384, 1180, 1021. ^1H NMR (300 MHz, DMSO-d_6): δ 9.91 (s, 1H), 9.13 (d, J = 2.1 Hz, 1H), 9.01 (d, J = 2.0 Hz, 1H), 8.63 (dd, J = 7.8, 1.0 Hz, 1H), 8.17 (dd, J = 7.8, 1.0 Hz, 1H), 7.16 (dd, $J = J$ = 7.8 Hz, 1H). ^{13}C NMR (75 MHz, DMSO-d_6): δ 159.4, 149.0, 146.1, 145.9, 142.2, 137.4, 136.9, 124.9, 124.6, 119.1, 85.1. HRMS/ESI: Calcd for $C_{11}H_6IN_3ONa$ $[M+Na]^+$ 345.9453, found 345.9455.

*5.1.6. 7-Iodo-5-(1-propylpiperidin-4-yl)methyloxypyrazino[2,3-c] quinoline (**14**)*

Starting from **13** (605 mg, 1.87 mmol) using general procedure C, **14** (589 mg) was obtained as a yellow powder. Yield: 68%. R_f (EtOAc/Et_3N (98:2)) = 0.18. Mp: 151–152 °C. IR (neat): ν (cm^{-1}) 2942, 2772, 1592, 1453, 1426, 1349, 1176, 1111, 1047. ^1H NMR (300 MHz, $CDCl_3$): δ 9.04 (d, J = 2.0 Hz, 1H), 8.97 (d, J = 2.0 Hz, 1H), 8.84 (dd, J = 8.0, 1.3 Hz, 1H), 8.29 (dd, J = 7.6, 1.3 Hz, 1H), 7.26 (dd, J = 8.0, 7.6 Hz, 1H), 4.70 (d, J = 6.8 Hz, 2H), 2.98 (d, J = 11.2 Hz, 2H), 2.43–2.12 (m, 3H), 2.03–1.92 (m, 4H), 1.63–1.39 (m, 4H), 0.88 (t, J = 7.4 Hz, 3H). ^{13}C NMR (75 MHz, $CDCl_3$): δ 158.3, 147.6, 145.5, 145.2, 143.5, 141.2, 130.8, 126.3, 124.4, 123.0, 100.5, 72.5, 60.9, 53.3 (2C), 35.0, 29.0 (2C), 19.9, 12.0. LC–MS (ESI): t_R = 5.41 min; $[M+H]^+$ 463.31. HRMS/ESI: Calcd for $C_{20}H_{24}IN_4O$ $[M+H]^+$ 463.0995, found 463.0993.

*5.1.7. 7-Tri(butyl)stannyl-5-(1-propylpiperidin-4-yl) methyloxypyrazino[2,3-c]quinoline (**15**)*

In a schlenk flash, under nitrogen, were introduced toluene (4.5 mL), water (0.3 mL), PPh_3 (9 mg, 5 mol%) and $Pd(OAc)_2$ (4 mg, 2.5 mol%). The mixture was heated at 50 °C for 20 min then **14** (150 mg, 0.32 mmol) in toluene (2.6 mL) and hexa-*n*-butylditin (0.25 mL, 0.49 mmol) were added. The mixture was heated at 90 °C for 16 h, filtered on celite, and evaporated *in vacuo*. The resulting oil was then purified by silica gel chromatography (eluent: Et_2O with 1% of Et_3N) to give **15** (91 mg) as a yellow oil. Yield: 45%. R_f (Et_2O/Et_3N (99:1)) = 0.58. IR (neat): ν (cm^{-1}) 2954, 2920, 1586, 1453, 1423, 1348, 1323, 1180, 1116. ^1H NMR (300 MHz, $CDCl_3$): δ 8.96 (d, J = 1.9 Hz, 1H), 8.88 (d, J = 1.9 Hz, 1H), 8.79 (dd, J = 7.9, 1.1 Hz, 1H), 7.84 (dd, J = 6.7, 1.1 Hz, 1H), 7.48 (dd, J = 7.9, 6.7 Hz, 1H), 4.48 (d, J = 7.0 Hz, 2H), 2.93 (d, J = 11.1 Hz, 2H), 2.28–2.19 (m, 2H), 2.11–2.00 (m, 1H), 1.97–1.90 (m, 4H), 1.56–1.41 (m, 10H), 1.31–1.09 (m, 12H), 0.84 (t, J = 7.3 Hz, 3H), 0.77 (t, J = 7.3 Hz, 9H). ^{13}C NMR (75 MHz, $CDCl_3$): δ 157.2, 149.2, 147.2, 146.4, 144.5, 143.3, 139.6, 130.9, 125.1, 124.2, 121.9, 72.0, 61.2, 53.4 (2C), 35.2, 29.3 (2C), 29.2 (3C), 27.4 (3C), 20.2, 13.7 (3C), 12.0, 10.2 (3C). HRMS/ESI: Calcd for $C_{32}H_{51}N_4OSn$ $[M+H]^+$ 627.3085, found 627.3091.

5.1.8. Radiosynthesis of [^{125}I]14

A 0.05 M NaOH (10 μL) solution containing 370 MBq of carrier -free $Na^{125}I$ (PerkinElmer) was added to a solution of precursor 15 (50 μg) in a mixture containing EtOH (10 μL), 1 M hydrochloric acid (10 μL), and 30% hydrogen peroxide solution (1 μL). After an incubation at room temperature for 20 min, [^{125}I]**14** was isolated by a gradient HPLC using a Bondclone C18 column (10 μm, 300 × 7.8 mm, Phenomenex) at 3 mL min^{-1} (10 mM H_3PO_4, 5–95% ACN over 10 min). HPLC was paired with a UV (Smartline UV Detector 200, Knauer) and radiodetector (GABI Star gamma flow monitor, Raytest) systems. The apparent specific activity was determined thanks to a calibration curve measured using growing amounts of the cold reference and to UV monitoring (254 nm) during the HPLC purification step. After collection, the product was concentrated by evaporation and formulated in saline. [^{125}I]**14** was isolated in a 88.7 ± 2.4% radiochemical yield and a specific activity of 61,050 ± 7844 GBq $mmol^{-1}$ (mean ± SD of 3 runs). Identification of [^{125}I]**14** was made a by comparison with the cold reference **14** by HPLC (see SI for HPLC data).

5.2. Biological evaluation

5.2.1. Pharmacological assay and screen

Binding of all compounds to native 5-HT_4R from guinea pig was determined using the method of Grossman [47].

For membrane preparations: male guinea pigs (300–350 g, Charles River) were subjected to euthanasia by cervical dislocation and decapitated. Brains were rapidly removed at 4 °C and striatal regions carefully dissected and pooled. The tissues were then suspended in 10 volumes of HEPES buffer 50 mM pH 7.4 at 4 °C. After homogenization at 4 °C (Ultra-Turrax, maximal speed, 15 s), and ultracentrifugation (23,000× *g*, 60 min, 4 °C), the pellet was resuspended in 10 volumes of HEPES buffer 50 mM pH 7.4 at 4 °C in

order to obtain a tissue concentration of about 100 mg of protein per mL. The protein concentration was determined by the method of Lowry [48] using bovine serum albumin as standard.

For radioligand binding studies: 600 μg of guinea pig membrane were incubated in duplicate at 37 °C for 30 min with [^{3}H]GR-113808 [47] (Perkin Elmer) and HEPES buffer 50 mM pH 7.4 at 37 °C. Incubation was terminated by rapid vacuum filtration through 0.5% polyethylenimine-presoaked Whatman GF/B filters (Alpha Biotech) using a Brandel Cell Harvester. Filters were subsequently washed three times with 4 ml of HEPES buffer 50 mM pH 7.4 at 4 °C. The method was first validated from saturation studies to determine the K_d and *Bmax*: 6 concentrations of [^{3}H]GR-113808 were used to give final concentrations of 0.02–0.8 nM, non-specific binding of [^{3}H]GR-113808 was defined in the presence of 30 μM serotonin. The K_d was calculated to 0.2 nM.

For competition studies with compounds **10a–o** and **14**, [^{3}H]GR-113808 was used to give a final concentration of 0.1 nM. Percentages of inhibition of the binding of [^{3}H]GR-113808 were obtained for two concentrations of the ligands to test (10^{-6} and 10^{-8} M).

For all of these compounds, affinity constants were calculated from 5-point inhibition curves using the EBDA-Ligand software, and expressed as $K_i \pm$ SD.

Other selected ligands **10g,l,m** and **14** were evaluated for binding to human 5-HT$_4$R. **14** was evaluated toward other serotonin receptors as well as for intrinsic activity at CEREP. Detailed assay protocols are available at the CEREP web site (http://www.cerep.com) under the following reference numbers. Binding assays: 5-HT$_{1a}$R (0131), 5-HT$_{1b}$R (0132), 5-HT$_{1d}$R (1974), 5-HT$_{2a}$R (0135), 5-HT$_{2b}$R (1609), 5-HT$_{2c}$R (0137), 5-HT$_3$R (0411), 5-HT$_{4e}$R (0501), 5-HT$_{5a}$R (0140), 5-HT$_6$R (0142), 5-HT$_7$R (0.144), SERT (0439). Functional assay: 5-HT$_{4e}$R (1045).

5.2.2. Lipophilicity evaluation

LogD at pH = 7.4 were measured by Techmed^{ill} (http://www.pcbis.fr/en/presentation-techmedill-en/) at the University of Strasbourg (France) for compound **5**, **6**, **10b–d**, **10f–m**, **10o** and **14** using chromatographic hydrophobicity index [41]. Calculated logD at pH = 7.4 were obtained using MarvinSketch 5.2.6 (http://www.chemaxon.com/products/marvin/marvinsketch/http://www.chemaxon.com/products/marvin/marvinsketch/).

5.2.3. SPECT imaging

While maintained under isoflurane anaesthesia (1.8–2.5% with pure oxygen) and installed in a U-SPECT-II imaging system (MILabs, The Netherlands), male Sprague Dawley rats (n = 3; 350–400 g) received a bolus injection in the tail vein with 38.9 ± 4.3 MBq of compound [^{125}I]**14** in 0.6 ml saline. Image frames of a length of 1 min were acquired for one hour following radiotracer injection. SPECT tomograms were reconstructed with a pixel ordered subsets expectation maximization algorithm (P-OSEM, 0.4 mm voxels, 4 iterations, 6 subsets) using MILabs proprietary software, and finally smoothed with a Gaussian filter of 0.6 mm FWHM. The SPECT images were analysed with PMOD software (PMOD Technologies, Zurich, Switzerland). The tomograms were coregistered to a reference MRI template of the rat brain [49] and the cerebral time activity curve were extracted in the cerebellum and in a group of limbic regions (comprising hippocampus, hypothalamus, amygdala, olfactory tubercles, septum, thalamus, and striatum). The conversion to percentage of injected dose and kBq mL^{-1} units was done using a phantom scan calibration. Immediately after the scan acquisition, rats were euthanized and their brain processed for autoradiography (see below).

5.2.4. Competition study by ex vivo autoradiography

Three Sprague Dawley rats (350–400 g) were anaesthetised with isoflurane (1.8–2.5% with pure oxygen), before receiving an injection in the tail vein with either 41.3 ± 0.6 MBq of compound [^{125}I]**14** alone or along with a dose of 1 mg kg^{-1} of **16** [44], a selective 5-HT$_4$R ligand. The animals were sacrificed by decapitation after 60 min, the brains were quickly removed and frozen in precooled isopentane at −20 °C. Brain of rats treated with [^{125}I]**14** alone or in combination with **16** were cut (20 μm-thick coronal sections) with a cryomicrotome (Leica) at −20 °C. The sections were mounted on glass slides, air-dried at room temperature and exposed to phosphor imaging plates overnight (Fuji Photo Film Co., Tokyo, Japan). Finally, the plates were scanned with a Fuji Bio-Imaging Analyzer BAS 1800II scanner (Fuji Photo Film Co., Tokyo, Japan), at 50 μm resolution to obtain *ex vivo* autoradiograms. The resulting autoradiograms were quantified using ImageJ software (http://rsb.info.nih.gov/ij), and specific binding ratios were determined as the ratio of intensity in target regions versus cerebellum, minus one.

Acknowledgements

The authors thank Dr. D. Harakat (Université de Reims Champagne Ardennes) for HRMS. This work has been partially supported by the “Réseau Crunch-Orga” (NF grant) and Région Haute Normandie. This work was also supported by the Swiss National Science Foundation (grant no. 310030_156829), the Geneva Neuroscience Centre, and the Ernst and Lucie Schmidheiny Foundation. The authors are grateful for the contributions of the Association IFRAD Suisse, which was created in 2009 at the initiative of the Fondation pour la Recherche sur Alzheimer (formerly IFRAD France).

Abbreviations

ACN	acetonitrile
Bs	brainstem
Cb	cerebellum
cc	corpus callosum
Cl	claustrum
Cx	cortex
Hip	hippocampus
inhbn.	inhibition
IP	interpeduncular nucleus
NM	not measured
PE	petroleum ether
S-Phos	2-dicyclohexylphosphino-2′,6′-dimethoxybiphenyl
St	striatum
Tu	olfactory tubercles

Appendix A. Supplementary data

Supplementary data related to this article can be found at http://dx.doi.org/10.1016/j.ejmech.2015.03.017.

References

[1] Y. Charnay, L. Léger, Brain serotonergic circuitries, Dialogues Clin. Neurosci. 12 (2010) 471–487.
[2] A. Dumuis, R. Bouhelal, M. Sebben, J. Bockaert, A 5-HT receptor in the central nervous system, positively coupled with adenylate cyclase, is antagonized by ICS 205 930, Eur. J. Pharmacol. 146 (1988) 187–188.
[3] A. Dumuis, R. Bouhelal, M. Sebben, R. Cory, J. Bockaert, A nonclassical 5-hydroxytryptamine receptor positively coupled with adenylate cyclase in the central nervous system, Mol. Pharmacol. 34 (1988) 880–887.
[4] H. Ouadid, J. Seguin, A. Dumuis, J. Bockaert, J. Nargeot, Serotonin increases calcium current in human atrial myocytes via the newly described 5-hydroxytryptamine4 receptors, Mol. Pharmacol. 41 (1992) 346–351.
[5] G.E. Torres, I.L. Holt, R. Andrade, Antagonists of 5-HT4 receptor-mediated responses in adult hippocampal neurons, J. Pharmacol. Exp. Ther. 271

(1994) 255–261.
[6] M. Maillet, S.J. Robert, M. Cacquevel, M. Gastineau, D. Vivien, J. Bertoglio, et al., Crosstalk between Rap1 and Rac regulates secretion of sAPPalpha, Nat. Cell. Biol. 5 (2003) 633–639.
[7] R. Bureau, M. Boulouard, F. Dauphin, F. Lezoualc'h, S. Rault, Review of 5-HT4R ligands: state of art and clinical applications, Curr. Top. Med. Chem. 10 (2010) 527–553.
[8] M. Camilleri, Serotonin in the gastrointestinal tract, Curr. Opin. Endocrinol. Diabetes Obes. 16 (2009) 53–59.
[9] F. De Ponti, M. Tonini, Irritable bowel syndrome: new agents targeting serotonin receptor subtypes, Drugs 61 (2001) 317–332.
[10] E. Qvigstad, T. Brattelid, I. Sjaastad, K.W. Andressen, K.A. Krobert, J.A. Birkeland, et al., Appearance of a ventricular 5-HT4 receptor-mediated inotropic response to serotonin in heart failure, Cardiovasc. Res. 65 (2005) 869–878.
[11] D.I. Leftheriotis, G.N. Theodorakis, D. Poulis, P.G. Flevari, E.G. Livanis, E.K. Iliodromitis, et al., The effects of 5-HT4 receptor blockade and stimulation, during six hours of atrial fibrillation, Europace 7 (2005) 560–568.
[12] T. Bach, T. Syversveen, A.M. Kvingedal, K.A. Krobert, T. Brattelid, A.J. Kaumann, et al., 5-HT 4(a) and 5-HT 4(b) receptors have nearly identical pharmacology and are both expressed in human atrium and ventricle, Naunyn. Schmiedeb. Arch. Pharmacol. 363 (2001) 146–160.
[13] M. Matsumoto, H. Togashi, K. Mori, K. Ueno, S. Ohashi, T. Kojima, et al., Evidence for involvement of central 5-HT(4) receptors in cholinergic function associated with cognitive processes: behavioral, electrophysiological, and neurochemical studies, J. Pharmacol. Exp. Ther. 296 (2001) 676–682.
[14] A. Meneses, E. Hong, Effects of 5-HT4 receptor agonists and antagonists in learning, Pharmacol. Biochem. Behav. 56 (1997) 347–3451.
[15] F. Lezoualc'h, 5-HT4 receptor and Alzheimer's disease: the amyloid connection, Exp. Neurol. 205 (2007) 325–329.
[16] S. Cho, Y. Hu, Activation of 5-HT4 receptors inhibits secretion of beta-amyloid peptides and increases neuronal survival, Exp. Neurol. 203 (2007) 274–278.
[17] A. Jean, G. Conductier, C. Manrique, C. Bouras, P. Berta, R. Hen, et al., Anorexia induced by activation of serotonin 5-HT4 receptors is mediated by increases in CART in the nucleus accumbens, Proc. Natl. Acad. Sci. U. S. A. 104 (2007) 16335–16340.
[18] G. Lucas, V.V. Rymar, J. Du, O. Mnie-Filali, C. Bisgaard, S. Manta, et al., Serotonin(4) (5-HT(4)) receptor agonists are putative antidepressants with a rapid onset of action, Neuron 55 (2007) 712–725.
[19] R.E. Gibson, H.D. Burns, T.G. Hamill, W.S. Eng, B.E. Francis, C. Ryan, Non-invasive radiotracer imaging as a tool for drug development, Curr. Pharm. Des. 6 (2000) 973–989.
[20] D.F. Wong, G. Gründer, J.R. Brasic, Brain imaging research: does the science serve clinical practice? Int. Rev. Psychiatry 19 (2007) 541–558.
[21] V.W. Pike, C. Halldin, K. Nobuhara, J. Hiltunen, R.S. Mulligan, C.-G. Swahn, et al., Radioiodinated SB 207710 as a radioligand in vivo: imaging of brain 5-HT4 receptors with SPET, Eur. J. Nucl. Med. Mol. Imaging 30 (2003) 1520–1528.
[22] A. Gee, L. Martarello, J. Passchier, M. Wishart, C. Parker, J. Matthews, et al., Synthesis and evaluation of [11C]SB207145 as the first in vivo serotonin 5-HT4 receptor radioligand for PET imaging in man, Curr. Radiopharm. 1 (2008) 110–114.
[23] R. Xu, J. Hong, C.L. Morse, V.W. Pike, Synthesis, structure-affinity relationships, and radiolabeling of selective high-affinity 5-HT4 receptor ligands as prospective imaging probes for positron emission tomography, J. Med. Chem. 53 (2010) 7035–7047.
[24] F. Caillé, T.J. Morley, A.A.S. Tavares, C. Papin, N.M. Twardy, D. Alagille, et al., Synthesis and biological evaluation of positron emission tomography radiotracers targeting serotonin 4 receptors in brain: [(18)F]MNI-698 and [(18)F] MNI-699, Bioorg. Med. Chem. Lett. 23 (2013) 6243–6247.
[25] A.A.S. Tavares, F. Caillé, O. Barret, C. Papin, H. Lee, T.J. Morley, et al., Whole-body biodistribution and dosimetry estimates of a novel radiotracer for imaging of serotonin 4 receptors in brain: [(18)F]MNI-698, Nucl. Med. Biol. 41 (2014) 432–439.
[26] B.R. Kornum, N.M. Lind, N. Gillings, L. Marner, F. Andersen, G.M. Knudsen, Evaluation of the novel 5-HT4 receptor PET ligand [11C]SB207145 in the Göttingen minipig, J. Cereb. Blood Flow. Metab. 29 (2009) 186–196.
[27] K. Varnäs, C. Halldin, V.W. Pike, H. Hall, Distribution of 5-HT4 receptors in the postmortem human brain – an autoradiographic study using [125I]SB 207710, Eur. Neuropsychopharmacol. 13 (2003) 228–234.
[28] L. Marner, N. Gillings, R.A. Comley, W.F.C. Baaré, E. Rabiner, A. Wilson, et al., Kinetic modeling of 11C-SB207145 binding to 5-HT4 receptors in the human brain in vivo, J. Nucl. Med. 50 (2009) 900–908.
[29] L. Marner, N. Gillings, K. Madsen, D. Erritzoe, W.F.C. Baaré, C. Svarer, et al., Brain imaging of serotonin 4 receptors in humans with [11C]SB207145-PET, Neuroimage 50 (2010) 855–861.
[30] K. Madsen, W.-J. Neumann, K. Holst, L. Marner, M.T. Haahr, S. Lehel, et al., Cerebral serotonin 4 receptors and amyloid-β in early Alzheimer's disease, J. Alzheimers. Dis. 26 (2011) 457–466.
[31] K. Madsen, L. Marner, M. Haahr, N. Gillings, G.M. Knudsen, Mass dose effects and in vivo affinity in brain PET receptor studies-a study of cerebral 5-HT4 receptor binding with [11C]SB207145, Nucl. Med. Biol. 38 (2011) 1085–1091.
[32] P.M. Fisher, K.K. Holst, B. Mc Mahon, M.E. Haahr, K. Madsen, N. Gillings, et al., 5-HTTLPR status predictive of neocortical 5-HT4 binding assessed with [(11)C] SB207145 PET in humans, Neuroimage 62 (2012) 130–136.
[33] E. Dubost, N. Dumas, C. Fossey, R. Magnelli, S. Butt-Gueulle, C. Ballandonne, et al., Synthesis and structure-affinity relationships of selective high-affinity 5-HT(4) receptor antagonists: application to the design of new potential single photon emission computed tomography tracers, J. Med. Chem. 55 (2012) 9693–9707.
[34] L.M. Paterson, B.R. Kornum, D.J. Nutt, V.W. Pike, G.M. Knudsen, 5-HT radioligands for human brain imaging with PET and SPECT, Med. Res. Rev. 33 (2013) 54–111.
[35] V.W. Pike, PET radiotracers: crossing the blood-brain barrier and surviving metabolism, Trends Pharmacol. Sci. 30 (2009) 431–440.
[36] W.A. Banks, Characteristics of compounds that cross the blood-brain barrier, BMC Neurol. 9 (Suppl. 1) (2009) S3.
[37] W.M. Pardridge, The blood-brain barrier: bottleneck in brain drug development, NeuroRx 2 (2005) 3–14.
[38] R.N. Waterhouse, Determination of lipophilicity and its use as a predictor of blood-brain barrier penetration of molecular imaging agents, Mol. Imaging Biol. 5 (2003) 376–389.
[39] J.S. Scott, A.M. Birch, K.J. Brocklehurst, A. Broo, H.S. Brown, R.J. Butlin, D.S. Clarke, Ö. Davidsson, A. Ertan, K. Goldberg, S.D. Groombridge, J.A. Hudson, D. Laber, A.G. Leach, P.A. MacFaul, D. McKerrecher, A. Pickup, P. Schofield, P.H. Svensson, P. Sörme, J. Teague, Use of small-molecule crystal structures to address solubility in a novel Series of G protein coupled receptor 119 agonists: optimization of a lead and in vivo evaluation, J. Med. Chem. 55 (2012) 5361–5379.
[40] N.A. Meanwell, Tactics in Contemporary Drug Design, Springer, 2014. ISSN 364255041X, 9783642550416.
[41] K. Valko, C. Du, C. Bevan, D. Reynolds, M. Abraham, Rapid method for the estimation of octanol/water partition coefficient (Log Poct) from gradient RP-HPLC retention and a hydrogen bond acidity term (Sigma alpha2H), Curr. Med. Chem. 8 (2001) 1137–1146.
[42] N. Fresneau, T. Cailly, F. Fabis, J.-P. Bouillon, Synthesis of substituted diazino[c] quinolin-5(6H)-ones, diazino[c]isoquinolin-6(5H)-ones, diazino[c] naphthyridin-6(5H)-ones and diazino[c]naphthyridin-5(6H)-ones, Tetrahedron 69 (2013) 5393–5400.
[43] E. Dubost, R. Magnelli, T. Cailly, R. Legay, F. Fabis, S. Rault, General method for the synthesis of substituted phenanthridin-6(5H)-ones using a KOH-mediated anionic ring closure as the key step, Tetrahedron 66 (2010) 5008–5016.
[44] S.S. Hegde, D.W. Bonhaus, L.G. Johnson, E. Leung, R.D. Clark, R.M. Eglen, RS 39604: a potent, selective and orally active 5-HT4 receptor antagonist, Br. J. Pharmacol. 115 (1995) 1087–1095.
[45] G. Paxinos, C. Watson, The Rat Brain in Stereotaxic Coordinates, fifth ed., Elsevier Academic, 2004.
[46] M.T. Vilaró, R. Cortés, G. Mengod, Serotonin 5-HT4 receptors and their mRNAs in rat and guinea pig brain: distribution and effects of neurotoxic lesions, J. Comp. Neurol. 484 (2005) 418–439.
[47] C.J. Grossman, G.J. Kilpatrick, K.T. Bunce, Development of a radioligand binding assay for 5-HT4 receptors in guinea-pig and rat brain, Br. J. Pharmacol. 109 (1993) 618–624.
[48] O.H. Lowry, N.J. Rosebrough, A.L. Farr, R.J. Randall, Protein measurement with the Folin phenol reagent, J. Biol. Chem. 193 (1951) 265–2675.
[49] W.K. Schiffer, M.M. Mirrione, A. Biegon, D.L. Alexoff, V. Patel, S.L. Dewey, Serial microPET measures of the metabolic reaction to a microdialysis probe implant, J. Neurosci. Methods 155 (2006) 272–284.